Thoracic Cancer ISSN 1759-7706

TECHNICAL NOTE

Enhancement of radiographic images in patients with lung nodules

Maher I. Rajab[1] & Ayman A. Eskandar[2]

1 Department of Computer Engineering, College of Computer and Information Systems, Umm Al-Qura University, Makkah, Saudi Arabia
2 Department of Radiology, College of Medicine, Umm Al-Qura University, Makkah, Saudi Arabia

Keywords
Frequency domain processing; lung cancer; lung nodules; X-ray enhancement.

Correspondence
Dr Maher I. Rajab, Department of Computer Engineering, College of Computer & Information Systems, Umm Al-Qura University, Abdiah Campus, Makkah, Saudi Arabia.
Tel: +966 2 527 0000 ext 3021
Fax: +966 2 528 1376
Email: mirajab@uqu.edu.sa

Received: 24 February 2011;
accepted: 20 March 2011.

doi: 10.1111/j.1759-7714.2011.00045.x

Abstract

Detection of lung nodules in a chest Radiograph is very difficult due to sensitivity to noise, lighting, and similar disturbances of the blood vessels and trachea. Therefore, such images need to be carefully examined to identify and characterize lung lesions. However, human interpretations are usually contradictory and may cause confusion. Current works propose an image processing technique based on frequency domain processing to clarify X-ray radiographic images taken in patients with a variety of lung lesions. The Picture Archiving and Communication Systems workstation allows transferring radiographic data from DICOM into JPEG image formats. In the preprocessing phase, the lung nodules are identified by an experienced chest radiologist and used for extracting regions of interest. Subsequently, low-pass followed by emphasis high-pass frequency filters are applied to enhance the images with appropriate cut-off frequencies. It has been found that high-frequency domain image filtering enhances the morphological features of lung masses. Enhanced images are then visually arbitrated by an expert radiologist. We found that the characteristics of lung lesions are easily identified after this process.

Lung cancer remains the most common cancer-related cause of death worldwide. Death subsequent to lung cancer alone outnumbers deaths from breast, prostate and colon cancers combined. According to the American Cancer Society, the overall 5-year survival rate is less than 15%. However when lung cancer is found in the early stages, the 5-year survival rate increases to more than 50%. Currently, only 15% of lung cancer is detected in the early, most treatable stages.

Chest radiography is the most frequently performed radiological imaging study and also one of the most challenging.[1] Although, chest radiograph can detect early lung cancer, as a new study from the National Cancer Institute (NCI) has illustrated, the false positive rate is still high. Furthermore, chest radiograph used for detecting lung cancer is the second most common cause for malpractice cases among radiologists as a result of observer errors including recognition, decision making and lesion conspicuity.

In the era of digital diagnostic radiography, denoising and enhancement have an important potential role in obtaining as much easily interpretable diagnostic information as possible without increasing the radiation dose to the patient.[2] Furthermore, due to the increasing usage of high resolution and high precision images with a limited number of human experts, the computational efficiency of the denoising and enhancement becomes more important.

Because of the large difference in the densities of the lung and other structures, the chest radiograph image uses a wide-range intensity distribution, which creates difficulty for focussing.[3,4] In this paper we propose an algorithm for the enhancement of chest radiographic images of lung lesions in patients with malignant and benign lung lesions for better detection, decision making, particularly in determining the growth rate of the nodule, and characterization of the disease.

Image processing techniques based on frequency domain analysis via Fourier transformation is proposed to enhance chest radiographic images of lung lesions. Our work methodology is formulated so that the suggested enhancement method applies the filtering in the frequency domain including low-pass filtering, basic high-pass filtering and high-frequency emphasis filtering.[5]

Previous work on nodule analysis

Early work by Carreira *et al.* proposed an algorithm for the enhancement of digitized radiographic images of chest.[6] The processing scheme adapted to the local information in the surroundings of each pixel that uses a priori knowledge of the signs indicating pathologies in the unprocessed images in order to achieve adequate enhancement. Preliminary work by Chiou *et al.* has been aimed at improving diagnostic accuracy and speed of lung cancerous pulmonary radiology using Hybrid Lung Nodule Detection (HLND) system.[7–9] Later Matozaki *et al.* proposed another method based on wavelet analysis to enhance and recognize regions of the mediastinum and lung on chest radiograph.[10] This enhancement method was applied to the digitized radiographs which make details of the mediastinum region in the original digitized (unprocessed) image not visible. Lung nodule detection methods for chest radiographs and CT scans have been the subject of some research.[11–16] The objective is always to find an automatic recognition system to identify and characterize lung lesions. Numerous methodologies have been proposed to verify this objective based on the different image processing techniques of genetic algorithms (GA),[11] and the neural networks[11–15] fuzzy logic system for lung nodule in digital images.[15] Among this research the enhancement of the lung nodules is addressed. Okada *et al.* proposed a solution to the problem of how to best represent the nodules numerically for various analysis tasks, this is the nodule characterization problem. [16]

Methodology

The block diagram given in Figure 1 indicates the main processing steps, which are followed in order to enhance the radiographic images for different chest lesions. Phase I of radiograph preprocessing consists of two steps that use size reduction of the radiograph Digital Imaging and Communication in Medicine (DICOM) data and manual selection of the region of interest (ROI) that includes the lung lesion(s). Phase II applies frequency domain filtering to enhance lung lesions in the selected ROI.

Compression of radiographic DICOM files

In order to simplify and speed up the Matrix Laboratory image processing, the radiograph images in DICOM standard are compressed into Joint Photographic Experts Group (JPEG) format.

As soon as the digital red, green and blue (RGB) images are prepared, manual selection made by an expert radiologist is applied to define the sufficient ROI window image that covers the desired lesion(s) in the high-resolution radiograph chest images. Processing a ROI window is advantageous to save time during image processing. Moreover, all images are subjected to gray-scale intensity. Eventually the images will be ready for the subsequent image processing procedures.

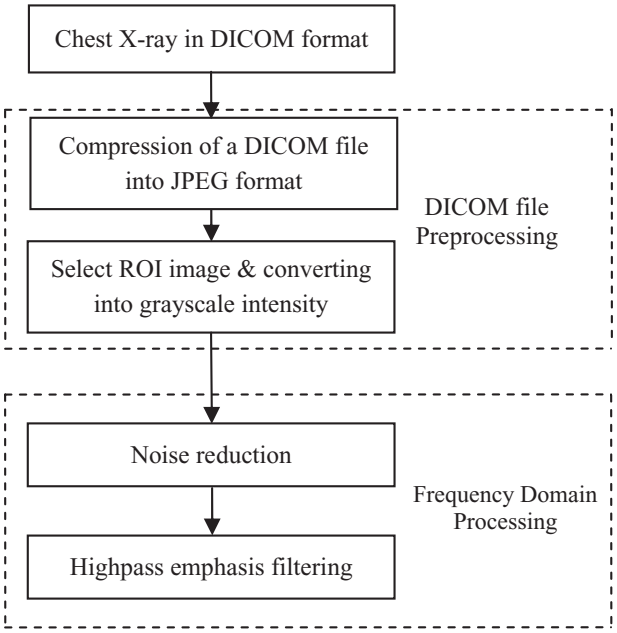

Figure 1 Steps used in image processing.

Frequency domain processing

We used frequency processing analysis via Fourier transformation to enhance X-ray radiographic images taken in patients with different lung lesions. The 2D, discrete Fourier transform (DFT), $F(u,v)$, of image $f(x,y)$ of size $M \times N$, is given by the equation

$$F(u,v) = \sum_{x=0}^{M-1} \sum_{y=0}^{N-1} f(x,y) e^{-j2\pi(ux/M+vy/N)} \quad (1)$$

Equation (1) represents the frequency domain which is simply the coordinate system spanned by $F(u,v)$ with u and v as (frequency) variables.[5] The foundation for linear filtering in both the spatial and frequency domains is the convolution theorem. If $H(u,v)$ represents filter function, then the convolution theorem may be written as:

$$f(x,y) * h(x,y) \Leftrightarrow H(u,v)F(u,v) \quad (2)$$

where $h(x,y)$ is the filter mask. The transfer functions of filters will be introduced in the following subsections. According to (2), the frequency domain filtering can be obtained by calculating the inverse Fourier transform of the right side of (2) that represents the required filtered image.

Noise reduction

The low-pass frequency filter will be used to reduce the noise of the image. Generally, three filters types will be examined in the image processing technique used in the present work namely: ideal; Butterworth; and Gaussian.

The transfer function of an ideal low-pass filter (ILPF) is represented as the following:

$$H_{lp}(u,v)=\begin{cases}1 & \text{if } D(u,v)\le D_0\\ 0 & \text{if } D(u,v)\ge D_0\end{cases} \quad (3)$$

where $D(u,v)$ is the distance from point (u,v) to the center of the filter $H_{lp}(u,v)$ and D_0 is a specified non-negative number. Accordingly, the locus of points $D(u,v)=D_0$ should be a circle. Figure 3a shows the perspective plot of the ideal low-pass filter with the cut-off $D_0=5$. As shown in Figure 3b, the filter $H_{lp}(u,v)$ is visualized by the image of circle diameter equal to $2D_0=10$. If the ideal filter in (3) multiplies by 0, or "cuts-off", the frequency components of the Fourier transform of the image will be outside the circle and also unchanged. On the other hand, if multiplied by 1, the frequency components will be inside the circle.

The transfer functions of Butterworth low-pass filter (BLPF) of order n, with a cut-off frequency at a distance D_0 from the origin is given by:

$$H_{lp}(u,v)=\frac{1}{1+[D(u,v)/D_0]^{2n}} \quad (4)$$

The transfer functions of Gaussian low-pass filter (GLPF) can be represented as the following equation:

$$H_{lp}(u,v)=e^{-D^2(u,v)/2\sigma^2} \quad (5)$$

where σ is the standard deviation. If it is assumed that $\sigma=D_0$, then the GLPF can be expressed in terms of the cut-off parameter D_0 as in the following:

$$H_{lp}(u,v)=e^{-D^2(u,v)/2D_0^2} \quad (6)$$

As shown in Figure 2, the BLPF and GLPF have smooth transfer function characteristics. In contrary, the cut-off frequency of the ILPF locus at points for which $H_{lp}(u,v)$ is down to a specified fraction of its maximum value. On the other hand, if $D(u,v)=D_0$ (6) indicates that the GLPF is down to $e^{-0.5}=0.607$ of its maximum amplitude value of 1.

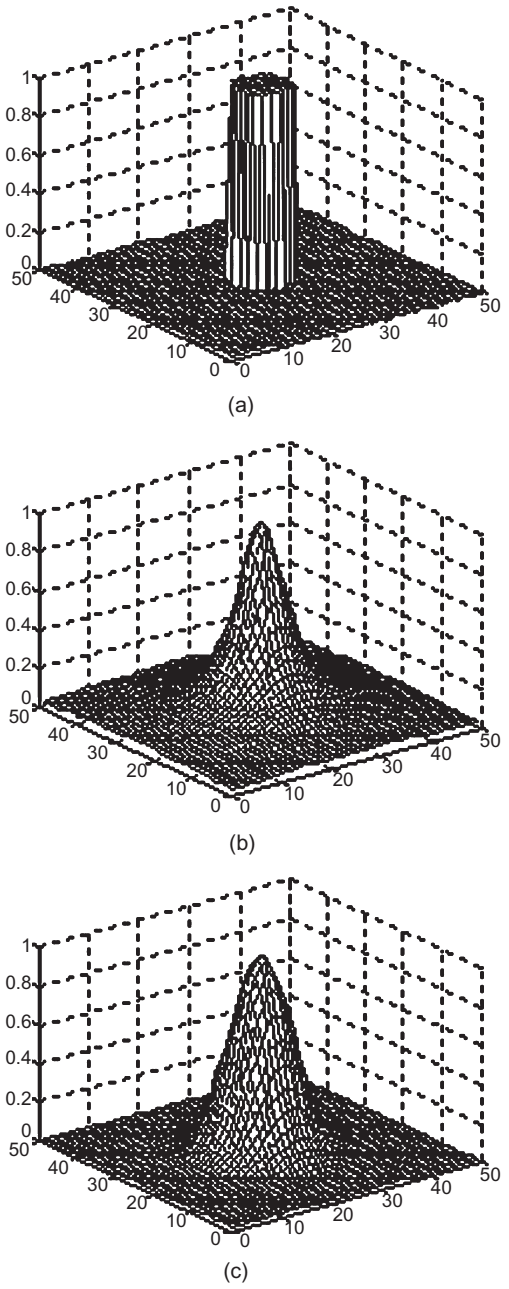

Figure 2 Perspective plots of low-pass filters using: (a) ideal (b) Butterworth, and (c) Gaussian transfer functions.

High-pass emphasis filtering

High-pass filtering is the essential primary step to enhance the image. Given the transfer function $H_{lp}(u,v)$ of a low-pass filter, the corresponding transfer function of the high-pass filter can be determined as the following:

$$H_{hp}(u,v)=1-H_{lp}(u,v) \quad (7)$$

As the high-pass filters reduce the average value of an image, the filtered image will lose most of the background tonality present in the original. In order to rectify this

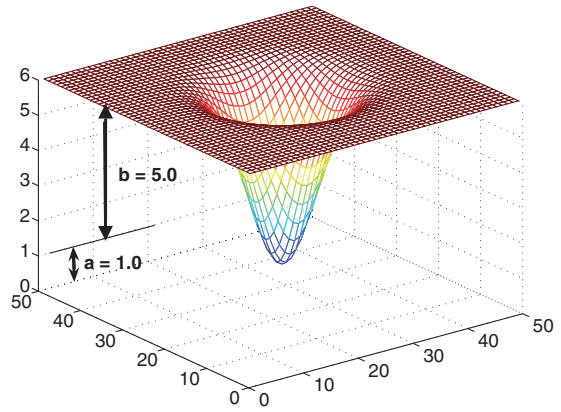

Figure 3 Gaussian high-pass emphasis filter: $a = 1.0$, $b = 5.0$.

problem, an offset can be added to a high-pass filter.[5] When the offset is combined with the product of the filter multiplied by a constant greater than 1, the approach is called high-frequency emphasis filtering. The emphasis filtering arises because the constant multiplier highlights the high frequencies. High-frequency emphasis has the transfer function as follows:

$$H_{hfe}(u,v) = a + bH_{hp}(u,v) \quad (8)$$

where a is the offset and b is the multiplier. Equation (8) demonstrates that the multiplier increases the amplitude of the low frequency's b, but the low frequency effects on enhancement are less than those due to high frequencies, as long as the offset is small compared to the multiplier. Figure 3 reveals the transfer function of the Gaussian emphasis high-pass filter with offset equals 1.0 and a multiplier of $b = 5.0$.

Results and discussion

The different filter types (i.e. ideal, Butterworth and Gaussian) are used for high-pass filtering given in (7) for the purpose of comparison and also to define which filter type is most suitable for the subsequent processing. Figure 4 illustrates the three high-pass filters (ideal, Butterworth, and Gaussian) when they are applied to the original radiograph image. The figure reveals that the Gaussian high-pass filter provides smooth transitions between various bands of intensities in an image. The effect of sharp discontinuities caused by the processed images due to ideal filtering is clearly visible, as shown in Figure 4b. It is also clear from Figure 4b–d that each image has lost most of the background tonality present in the original image. The processing steps method described in Table 1 is applied to the radiograph images of different lung lesions. In these experiments the expert radiologist visually determined the best enhancement to assure lesion conspicuity and subsequently determine the growth rate of the nodule and characteristics of the lesion border in various lung images. Various runs of the algorithm show that the best offset value, a, of the Gaussian emphasis high-pass filtering is a = 1.0, Equation 8, and the multiplier constant, b, is found to be best set to the value of 5. The cut-off frequency of high-pass filtering, f_{ch}, is kept to equal 0.05 and of low-pass filtering, f_{cl}, is kept to equal 0.25.

Table 1 Processing steps to enhance X-ray radiographic images

Step1: Compression of high-resolution radiographic DICOM file:
- Compress DICOM file to JPEG image $f(x,y)$,
- Select a region of interest image $f_{ROI}(x,y)$ from $f(x,y)$,
- Create a gray-scale intensity image $f_{gy}(x,y)$ from a red, green and blue image $f_{ROI}(x,y)$

Step 2: Noise reduction
- Apply Gaussian low-pass frequency filtering,
- Set cut-off frequency, f_{cl},
- Compute the inverse fast Fourier transform to obtain the corresponding filtered image: $f_{lp}(x,y) = FFT^{-1}(H_{lp}(u,v)F(u,v))$

Step 3: X-ray image enhancement
- Apply Gaussian high-pass frequency emphasis
- Filter image $f_{lp}(x,y)$; output of *Step 2:*
- Set cut-off frequency, f_{ch}
- High frequency emphasis filtering: $H_{hfe}(u,v) = a + bH_{hp}(u,v)$
- Compute the inverse fast Fourier transform to obtain the corresponding filtered image: $f_{gy}(x,y) = FFT^{-1}(H_{hfe}(u,v)F(u,v))$

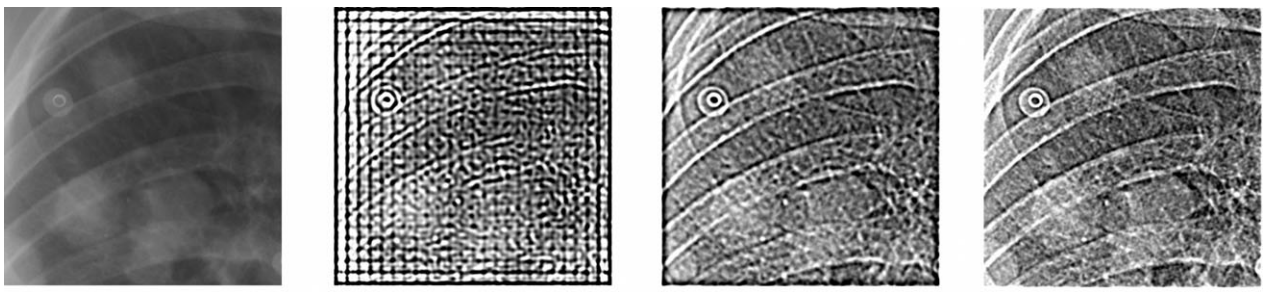

Figure 4 Applying high-pass filters to low-resolution a image containing porosities. (a) Original radiograph image. (b) Ideal high-pass filter; (c) Butterworth high-pass filter; and (d) Gaussian high-pass filter.

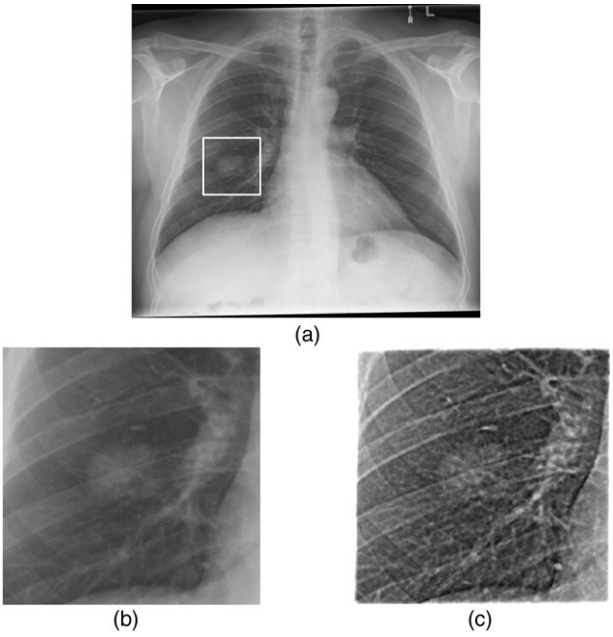

Figure 5 (a) Chest radiograph of a lung. (b) Region of interest selected from the right lung in image (a) with benign lesion. (c) Enhanced image in (b).

The image processing procedures given in Table 1 were applied to images of chest radiographs, as shown in Figures 5–7, with the best enhancement parameters of both filters according to the optimum offset value, *a*, multiplier, *b*, and cut-off frequencies of the two filters. It has to be mentioned that the low-pass filtering was applied at its low parameters considering the high-resolution of the chest radiograph images obtained with the new digital radiograph technology.

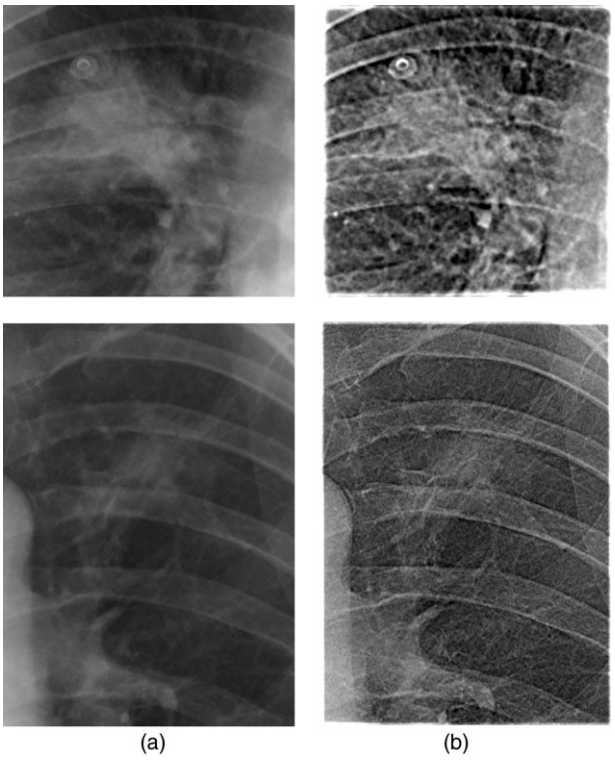

Figure 7 (a) Region of interest of radiograph images selected from patient with malignant lesions. (b) Enhanced images in (a).

The original images given in Figures 5a, 6a,7a for the benign and malignant lesions were developed into very clear enhancement images as shown in Figures 5b, 6b, 7b. Figure 5a illustrates an example of a lung nodule identified by an experienced chest radiologist, and is used for extracting the ROI as

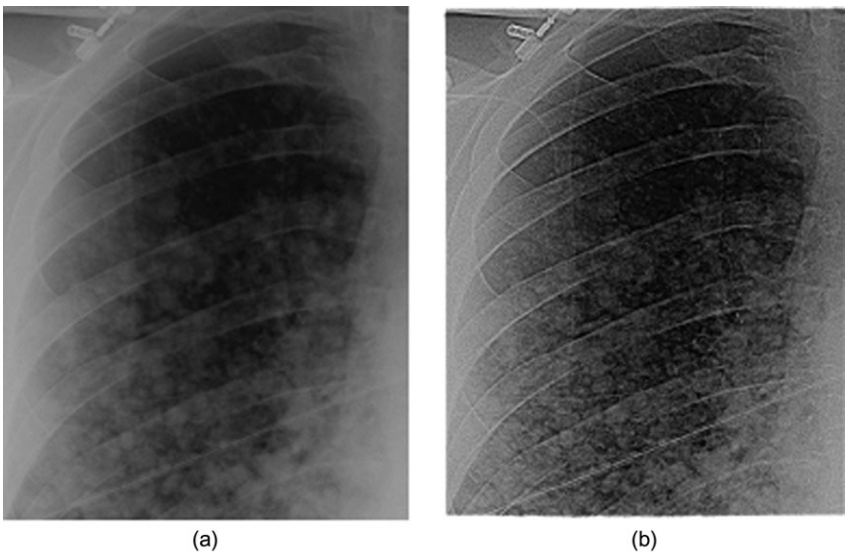

Figure 6 (a) Region of interest of radiograph images selected from patient with benign lesions. (b) Enhanced image in (a).

shown in Figure 5b. Figure 5c shows the final enhanced lesion which demonstrates a well-defined, rounded smooth border, in spite of the overlying pulmonary vessels that were crossing the lesion and obscuring its borders in the pre-enhanced image. After the enhancement and the review by the radiologist the lesion was thought to be most likely benign in nature giving the patient's clinical history and the lesion's morphological characteristics. This was further confirmed pathologically to be histoplasmosis (benign) after a needle biopsy of the lesion. In contrast, the enhanced malignant lesion shown in Figure 7b demonstrates clearly the shaggy irregular border, in spite of the overlying ribs, which were partially obscuring the lesion on the pre-enhanced image. This lesion was also confirmed pathologically after a CT-guided biopsy to be a malignant lung cancer. This comprehensibility removes confusion surrounding the identification of the lesion. If expert eyes, (i.e. the radiologist's), examine images they can give a definitive diagnosis,. Our results can only be attributed to the frequency domain processing via Fourier transformation that is used in the image processing enhancement procedures are used in the present work. This image processing technique not only helps radiologists to make correct decisions during radiograph sessions but may also enhance radiograph accessibility to other chest diseases in the field of the automatic recognition system to identify and classify the types of chest lesions, benign or malignant.

Conclusions

The following conclusions can be deduced:

- GLPF is essential to reduce the noise background.
- Gaussian emphasis high-pass filtering usage enhances the lung nodules for better detection and morphological characterization.
- Best enhancement results for images can be expected when offset, a, equals 1.0, multiplier, b, equals 5 and high-pass filtering, f_{ch}, equals 0.05, and the low-pass filtering, f_{cl}, equals 0.25.
- Generally, the misleading factors usually expected during the interpretation of radiograph images of lung lesions, can be beaten by using frequency domain processing analysis via the Fourier transformation technique due the excellent enhancement of the radiograph images of different benign and malignant lesions.

Acknowledgements

The authors would like to thank UA Hospital, Edmonton, Canada, for their support providing the radiograph lung cancer images, which facilitated the work in this study.

Disclosure

No authors report any conflict of interest.

References

1 MacMahom H, Vyborny C. Technical advances in chest radiography. *AJR* 1994; **163**: 1049–59.
2 Oktem H, Egiazarian K. An approach to adaptive enhancement of diagnostic X-ray images. *EURASIP J Appl Signal Processing* 2003; **5**: 430–6.
3 Liu H, Nodine CF, Miller WT. Edge enhancement to improve visualizations of tube/line placement in x-ray imaging. Medical Imaging 1995 Proceedings of SPIE Vol. 2434.
4 Hariharan S, Ray AK, Ghosh MK. An algorithm for the enhancement of chest X-ray images of tuberculosis patients. *Proc IEEE Int Conf Ind Technol* 2000; **1**: 107–12.
5 Gonzalez RC, Woods RE, Eddins SL, eds. *Digital Image Processing Using MATLAB*, 4th edn. Pearson Prentice Hall, Upper Saddle River 2004; 108–40.
6 Carreira MJ, Cabello D, Mosquera A, Penedo MG, Facio I. Chest X-ray image enhancement by adaptive processing. Proceedings of the Annual International Conference of the IEEE Engineering in Medicine and Biology Society, Vol. 13: 1991.
7 Chiou YSP, Lure YMF, Ligomenides PA. Neural network image analysis and classification in hybrid lung nodule detection (HLND) system. Proceedings of the IEEE-SP Workshop, pp. 517–26, 1993.
8 Chiou YSP, Lure YMF, Ligomenides PA, Fritz S. Application of neural network based hybrid system for lung nodule detection. Proceedings of Sixth Annual IEEE Symposium on Computer-Based Medical Systems, pp. 211–16, 1993.
9 Chiou YSP, Lure YMF, Ligomenides PA. Neural-knowledge base object detection in Hybrid Lung Nodule Detection (HLND) system. IEEE International Conference on Neural Networks, vol. **7**, 1994.
10 Matozaki T, Tanishita A, Ikeguchi T. Image enhancement of chest radiography using wavelet analysis. Proceedings of the 18th Annual International Conference of the IEEE Engineering in Medicine and Biology Society, vol. 3, pp. 1109–10, 1996.
11 Hara T, Fujita H, Yongbum L, Yoshimura H, Kido S. Automated lesion detection methods for 2D and 3D chest X-ray images. Proceedings. International Conference on Image Analysis and Processing, 1999.
12 Suzuki K, Feng L, Sone S, Doi K. Computer-aided diagnostic scheme for distinction between benign and malignant nodules in thoracic low-dose CT by use of massive training artificial neural network. *IEEE Trans Med Imaging* 2005; **24**: 1138–50.
13 Suzuki K, Zhenghao S, Jun Z. Supervised enhancement of lung nodules by use of a massive-training artificial neural network (MTANN) in computer-aided diagnosis (CAD). 19th International Conference on Pattern Recognition, pp. 1–4, 2008.
14 Jinzhu Y, Yang L, Wei L, Dazhe Z. A three-dimensional method for detection of pulmonary nodule. 2nd International

Conference on Biomedical Engineering and Informatics, BMEI '09, pp. 1–4, 2009.
15 Hosseini R, Dehmeshki J, Barman S, Mazinani M, Jouannic AM, Qanadli S. A fuzzy logic system for classification of the lung nodule in digital images in computer aided detection. ICDS '10 Fourth International Conference on Digital Society, pp. 255–59, 2010.
16 Okada K, Comaniciu D, Krishnan A. Robust anisotropic Gaussian fitting for volumetric characterization of Pulmonary nodules in multislice CT. *IEEE Trans Med Imaging* 2005; **24**: 409–23.